JOINT EUROPEAN TORUS

JET–P(92)25

W.G. Core, G.A. Cottrell
and JET Team

Fast Ion Current Density Profile in a Tokamak with Symmetric-Launch Ion Cyclotron Resonance Heating

Fast Ion Current Density Profile in a Tokamak with Symmetric-Launch Ion Cyclotron Resonance Heating

W.G. Core, G.A. Cottrell
and JET Team*

JET-Joint Undertaking, Culham Science Centre, OX14 3DB, Abingdon, UK

* *See Annex*

Preprint of Paper to be submitted for publication in
a letter in Nuclear Fusion

FAST ION CURRENT DENSITY PROFILE IN A TOKAMAK WITH SYMMETRIC-LAUNCH ION CYCLOTRON RESONANCE HEATING

W.G. Core and G.A. Cottrell
JET Joint Undertaking, Abingdon, Oxon., OX14 3EA, UK

ABSTRACT

Two-ion ICR (Ion Cyclotron Resonance) heating in a tokamak can produce superthermal minority ions having orbital radii comparable with the plasma radius. The drift motion causes the trapped fast ions to precess around the torus, thus forming a fast ion current. We have used a semi-analytical model and a Monte-Carlo RF orbit code to calculate the direction, magnitude and profile of this current. For typical high power central ICR heating of JET, we find a fast ion current density of $j_{||} \sim 0.7MAm^{-2}$, peaked at a radius ~ 30cm from the centre where it enhances the local current density. The effect of the fast ion current is to flatten the q-profile within the region of the inversion radius of MHD sawteeth, where sawtooth stability is expected theoretically to be sensitive to the radial profile of current density. The fast ion current could explain the observed sawtooth stabilisation during ICRH. We have examined RF heated JET data for evidence of a correlation between the natural duration of sawtooth-free periods and the expected magnitude of the off-axis fast ion current density. The data show a threshold current density below which sawteeth are not stabilised. Above this threshold, the duration of sawtooth-stable periods increases monotonically with the magnitude of the off-axis RF fast ion current density.

The use of high power radio frequency heating in the ion cyclotron range of frequencies offers one of the most promising methods of heating tokamak plasmas to thermonuclear temperatures. The damping of the fast magnetosonic wave on a minority ion species leads to the development of a non-Maxwellian velocity distribution function which is highly anisotropic with a significant fraction of the resonating ions trapped in the toroidal magnetic field [1]. In the large tokamaks currently operating (JET, TFTR) in which the wave fields are strongly focussed on or near the magnetic axis, resonant ions in the MeV range of energies are produced. These ions have large Larmor radii, and those particles which move on banana or D-shaped orbits passing close to the centre of the discharge make large radial excursions across the minor radius of the torus. The maximum radial excursion of such an orbit [2] is given by,

$$r_{max} \cong R_0 (2.9 \rho q / R_0)^{2/3}, \quad (1)$$

where the tokamak safety factor is $q = rB_\phi/RB_\theta$, B_ϕ, B_θ are the toroidal and poloidal magnetic fields respectively, the Larmor radius in the total magnetic field is $\rho = v_\perp/\omega_{ci}$ and the gyrofrequency is $\omega_{ci} = Z_f B_\phi / M_f$. The heated particles have atomic number Z_f and mass $M_f = A_f m_p$, and $v_\perp$ is the perpendicular velocity of the ion. As an example, consider a typical helium-3 minority ion with perpendicular energy 3 MeV in JET having Larmor radius $\rho = 0.06$ m, and perpendicular velocity $v_\perp \cong 10^7$ m s^{-1}. The maximum radial excursion of the ion from the resonance layer is $r_{max} \cong 0.5$ m, and the maximum parallel velocity at this point is $v_\parallel \cong 5\ 10^6$ m s^{-1}. On the outer (large radius) branch of the orbit, the parallel velocity $v_\parallel$ is large and positive but on the inner (small radius) branch it is smaller and negative. In the limit of negligible poloidal Larmor radius ($\rho_\theta \sim 0$), the positive and negative motions exactly cancel in one orbital period resulting in no net parallel motion. However, with finite poloidal Larmor radius, these motions no longer cancel and, as is well known, the orbit as a whole precesses around the torus [3]. Considering the whole ensemble of heated minority ions, this motion gives rise to a net diamagnetic current of fast ions in a direction having the same sense as the plasma current.

From the point of view of local current generation, simple consideration of the net precessional motion of the fast ions neglects significant variations in the parallel velocity around the ion orbit. For fast ions having large poloidal Larmor radii, the ion current density is enhanced in a local region of the mid-plane outer orbital segment where $v_{//}$ is large and positive. However, as the ions drift back between their turning points along the inner segments of their orbits, $v_\parallel$ is smaller and negative. On general grounds we would therefore expect the fast ion current density to have inner negative and outer positive components on a radial scale of length $\sim \rho_\theta$. Moreover, when the poloidal Larmor radius becomes comparable with the scale length of the current density profile, we expect the fast ion current density to modify that of the underlying inductive current. For a sufficiently large off-axis fast ion current density, there will be a flattening of the current profile inside a region of radius $\sim \rho_\theta$.

In this letter we discuss first the radial structure of the diamagnetic fast ion current, using a simple semi-analytical model. Then we calculate its magnitude and radial density profile using the HECTOR Monte-Carlo code [4] and consider the effect of the diamagnetic current on the q-profile. Finally, we derive a scaling law for the off-axis fast ion component and use it to examine JET data for evidence of the possible role played by the fast ion current in stabilising MHD sawteeth.

To obtain an initial estimate of the magnitude and spatial distribution of the current density carried by the centrally heated minority ions, we have used a semi-analytical model, based on solution of the the guiding-centre orbit equation to calculate the fast ion current at points (ε, θ) in the poloidal plane where $\varepsilon = r / R$ is the inverse aspect ratio and θ the poloidal angle. A gaussian RF deposition profile was used and the background density and electron temperature profiles were assumed to be of parabolic form. The fast ion energy distribution function was approximated by a Stix minority tail in the high energy limit, as discussed in Ref. [5]. For a set of typical JET parameters (Table I), the result of this calculation is shown as a contour map in Fig.1. The particles are reflected at the resonance line ($r = 0$) and so do not penetrate to the high field side of it. The fast ion current is therefore poloidally asymmetric with respect to $r = 0$. The map shows a prominent semi-circular ridge of positive (co-directed) current density which results from the accumulation of co-moving ions on the outer part of their orbits. The two small positive bumps at test points near the ends of the ridge result from the relatively longer time spent by the particles as they approach their turning points. Closer to the centre, the net current is negative and arises from the returning paths of the particles.

A poloidally asymmetric, non-inductive current density profile of the form shown in Fig.1 will modify the tokamak equilibrium, particularly in the central region where the magnitude of the fast ion current density can be comparable to the inductive current density. A full solution to the equilibrium problem, with force balance satisfied everywhere, is beyond the scope of the present paper. However, we expect there to be an outward shift of the magnetic axis, since there is a net positive current on the low field side of the resonance. Based on the JET parameters assumed in this letter, we estimate the first moment (centroid) of the current distribution to be displaced $\Delta R \sim 5$ cm outwards.

The fast ion current profile has also been calculated using the Monte-Carlo code HECTOR. This code follows the guiding centre trajectories in the confinement field of the tokamak and includes the important Coulomb scattering processes of energy diffusion, dynamical friction, pitch angle scattering, and the resonant interaction of the ions with the wave field. Further details on the treatment of the interaction with the background plasma and cyclotron wave fields can be found in Ref [4]. These effects were not included in the simple semi-analytical model. The plasma was assumed to be in steady state, with background densities and temperatures of the form,

$$n(\psi) = \{n(0) - n(1)\}(1 - \psi)^{\alpha} + n(1), \qquad (2)$$

where ψ is the poloidal flux function, α the profile parameter, and (1), (0) are the edge and central values respectively. The RF power absorption profile was taken to be,

$$P(Z) = P(0)\ exp(-2LZ^2), \tag{3}$$

where Z is the distance from the median plane along the cyclotron resonance layer, and L the electric field decay parameter. Based on full-wave calculations of the fast wave damping in JET geometry [6], the characteristic decay length is typically $L = 0.2$ m. Single pass absorption was assumed with a fixed wave vector parallel to the magnetic field. The minority ions were assumed to be Maxwellian with temperature equal to that of the bulk species and distributed uniformly over the inner region of the torus $0 \leq \psi \leq 0.6$. To achieve a reasonable degree of confidence in the calculation of the current density 4000 particle trajectories were followed until a steady state of constant fast ion tail temperature was reached. The resultant fast ion current density profile, calculated after t = 3.0 seconds of heating and averaged over the displaced flux surfaces (at $R = R_0 + \Delta R$) is shown in Fig.2 for the typical JET parameters given in Table I. This heating time is equivalent to approximately three times the ion-electron momentum slowing-down time (evaluated in the plasma core) and was found to be adequate to ensure that the energetic ions reached steady-state. The maximum fast ion current density $j_{||} \sim 0.7 MA/m^2$ is parallel to the plasma current and occurs at minor radius 0.3 m. The current density curve has a zero at radius $r_0 = 0.14$ m. In the Monte-Carlo calculation, integration of the profile from r = 0 to $r = r_0$ gave the negative component of the fast ion current $I_- = -16$ kA, and integration from $r = r_0$ to r = a gave the positive component, $I_+ = +200$ kA; the net co-current is $I_f = I_- + I_+ = +184$ kA. The semi-analytic model is compared in Fig.2 and shows reasonable agreement considering that, in that case, a simplified minority distribution function was used.

The non-inductive fast ion current will modify the initial current density and the resulting q-profile. To calculate the effect on the q-profile we model the fast ion current density by a superposition of functions of the form

$$A\psi^p\ exp\text{-}q\psi^{1/2}, \tag{4}$$

where A, p, and q are chosen to fit the calculated current density profile. The results for the initial current density profile $j = j(0)(1 - \psi)^\alpha$, where $j(0)$ is chosen to yield a fixed edge safety factor $q(a) = 2.4$, and $\alpha = 5/2$ is used to give the experimentally observed $q(0) \sim 0.7$ are shown in Fig. 2. The q-profile is modified considerably, the on-axis value $q(0)$ increasing from 0.75 to 1.33, and the profile becomes non-monotonic with the appearance of a local minimum, $dq/dr = 0$ within the $q = 1$ radius.

The fast ions also transfer momentum to the thermal electrons which gives rise to a back-electron current opposing that of the fast ions. By analogy with the standard treatment of this

effect in calculations of the neutral beam driven current [7], the net RF-driven current density is given by,

$$j_{RF} = j_{\|}\left(1-\frac{Z_f}{Z_{eff}}(1-1.46\varepsilon^{1/2}A)\right), \tag{5}$$

where the effective charge number of the plasma is Z_{eff}, and the parameter A is of the order unity [8]. The right-hand term allows for the fact that electrons, trapped in the toroidal field gradient, cannot contribute to the back-electron current. The term partly ameliorates the effect of the back-electron current, particularly at large values of ε. With the inclusion of the back electron current Eq. (5) with $Z_f = 2.0$, $Z_{eff} = 3.5$, and $A = 1$, the non-inductive current density maximum at r = 0.3 m is reduced to $j_{\|} \sim 0.44MA/m^2$, and q(0) = 1.05. Nevertheless the increase in $q(0)$ above unity as well as the flattening of the q-profile within the inversion radius may give rise to observable effects, particularly in the context of equilibrium, stability and the suppression of sawtooth activity. Therefore we have examined experimental data, from JET ICR heated discharges, for evidence of sawtooth suppression when the predicted diamagnetic fast ion current is expected to be significant.

To do this, we have derived a scaling-law for a quantity proportional to the magnitude of the off-axis positive peak of the RF driven ion current. This quantity could be evaluated using experimental parameters. At the point of maximum radial excursion of the fast ion orbit ($\varepsilon_{max} = r_{max}/R$), the maximum parallel velocity is given approximately by,

$$v_{\|max} \approx v\varepsilon_{max}^{1/2}. \tag{6}$$

At the radius of the positive peak of the RF driven ion current, the net local fast ion current density will therefore scale with plasma parameters as,

$$j_{\|} \alpha\, nZ_f v\, \rho_\theta^{1/3}, \tag{7}$$

where n is the number density of fast ions.

In searching for evidence of possible RF-driven fast ion current effects in JET data, we have considered the effect that the fast ion off-axis current might have on the duration of sawtooth-free periods in RF centrally heated minority ion discharges. The normal criterion [9] for a JET discharge to contain a sawtooth-free period is that sawtooth activity should cease for a time greater than 0.6 sec. Although this criterion is somewhat arbitrary, it does however,

clearly separate sawtoothing and sawtooth-stable JET discharges. The criteria used to select JET discharge data are listed below. We have only analysed discharges where:

1) the data was taken during the flat-top phase of the plasma current,
2) the plasma was not evolving dynamically,
3) only ion cyclotron resonance minority heating was applied with steady state total coupled RF power,
4) the cyclotron resonance position was closer than 0.15m from the magnetic axis,
5) the sawtooth-free periods chosen terminated spontaneously (i.e. the termination was not caused by switching of the RF power, plasma disruption or other event).

The data span ranges in plasma current and toroidal field respectively of $2.0MA \leq I_p < 3.5MA$ and $3.1T \leq B_\phi < 3.45T$ with coupled RF power $P_{rf} < 14.6MW$. In our comparison of JET sawteeth with the calculated fast ion current scaling law, Eq. (7), we note the explicit dependence on the fast ion density, n. In JET hydrogen minority heating experiments, there is always a small residual hydrogen component present which introduces uncertainties in the analysis of that data. Therefore we have chosen to analyse only discharges with ^{3}He minority heating. In these, known quantities of the minority gas were injected into the plasma prior to the application of RF heating from which the ^{3}He concentration was determined.

The average velocity of the minority ions was estimated using the measured anisotropic component of the total energy of the fast ions, $W_f = 4/3(W_{dia} - W_{mhd})$, where W_{dia} is the plasma energy measured diamagnetically and W_{mhd} the plasma energy calculated from equilibrium. In the dataset analysed the largest value of W_f was 1.3 MJ with an estimated error of 0.2 MJ. The average velocity of the fast ions having this value of W_f is typically $v \cong 10^7$ m s^{-1}. In Fig. 4, we show a correlation plot of the measured durations of sawteeth and sawtooth-free periods as a function of the scaling law for the off-axis RF-driven current. As can be seen, there is a non-linear and positive correlation. In addition, there appears to be a threshold in the fast ion current density above which sawteeth become stable.

To conclude, we have examined the possibility that large fast ion currents are produced during ICRF heating. These currents, which are similar to those discussed in Ref. [10] arise because the fast ions are preferentially trapped in the toroidal field gradients and make large radial excursions across the minor radius of the torus. Simple particle orbit considerations indicate two regions of current concentration, a positive current in the direction of the discharge current and close to the MHD sawtooth inversion radius and a negative return current near the axis of the discharge. A Monte-Carlo study of a typical JET discharge indicates that significant ion currents are generated during ICRH. We find a co-current density maximum of

$j_{||} \sim 0.7 MA/m^2$ and a counter-current density maximum of $j_{||} \sim -0.2 MA/m^2$. These non-inductive currents give rise to a significant modification of the q-profile, and for the particular current profile considered the on-axis safety factor $q(0)$ is increased from 0.7 to a value lying in the range of $1 < q(0) < 1.3$, and a flattening of the q-profile within the inversion radius, where $dq/dr = 0$. Furthermore, these fast ion currents could explain the observed sawtooth stabilisation during ICRH. To investigate the effect on stability we have found an anti-correlation in JET data between the sawtooth-stable period and the magnitude of the fast ion current. We note that, experimentally, it is found to be extremely difficult to make long sawtooth-free periods when the distance between the cyclotron resonance position and the magnetic axis is larger than approximately 0.4 m [9]. This observation is consistent with the present model because, when the resonance position is moved off-axis, the average energy of the minority ions is reduced. Consequently the average poloidal Larmor radii are decreased and so is the off-axis fast ion current density. In experiments with neutral beam heating, the sawtooth periods are small. This observation is also consistent with the present mechanism because the average energy of the injected beam ions is generally much smaller than that of the ICR heated minority ions. Thus the average poloidal Larmor radii are smaller than for ICR heating and therefore the off-axis current density is relatively small. The (few) instances where NBI has been observed to result in sawtooth-stable periods may, possibly, be due to an off-axis peaking of the beam-driven current.

There are several MHD models which have been put forward to explain sawtooth stabilization with kinetic effects [11-13]. In these the sawtooth is stabilized by the radial pressure gradient of the fast ions. In support of the model considered in this letter, we stress the relatively simple basis of the fast ion current which may be able to perturb significantly the central part of the q-profile. A clear experimental prediction, therefore, is a flattening of the q-profile near the sawtooth inversion radius. Millimetre-wave Faraday rotation measurements have been used previously to determine the q-profile on JET [14]. However, interpretation of the these line-integrated interferometer data depend critically on a prior knowledge of the structure of the magnetic surfaces. If, as we suggest above, the equilibrium is perturbed by the presence of the fast ion current, then only a modified equilibrium should be used in order to obtain a consistent interpretation of the experimental data. Further areas of theoretical work include a self-consistent treatment of the tokamak equilibrium in the presence of the fast ion current, MHD stability and the complex magnetic structure implied by the poloidally asymmetric current.

ACKNOWLEDGEMENTS

It is a pleasure for the authors to thank Drs. J.W. Connor, J. Hugill, J. Jacquinot, D.F.H. Start and T.E. Stringer for discussions, and M. Kovanen for assistance with running the HECTOR code.

REFERENCES

[1] STIX, T.H., Nuclear Fusion **15** (1975) 737.

[2] STRINGER, T.E. (1974) Plasma Physics 16, 651.

[3] MIYAMOTO, K., *Plasma Physics for Nuclear Fusion*, MIT Press, Cambridge, Mass., USA (1980) 70.

[4] KOVANEN, M.A., CORE, W.G., HECTOR: A code for the study of charged particles in axisymmetric tokamak plasmas, JET-P(90)40.

[5] COTTRELL, G.A. and START, D.F.H., Nuclear Fusion **31** (1) (1991) 61.

[6] ERIKSSON, L-G., HELLSTEIN, T., BOYD, D.A., et al., Calculations of power deposition and velocity distributions during ICRH: Comparison with experimental results, Nuclear Fusion **29** (1989) 87.

[7] CONNOR, J.W. and CORDEY, J.G., Nuclear Fusion **14** (1974) 185.

[8] START, D.F.H., CORDEY, J.G. and JONES, E.M., Plasma Physics **22** (**4**) (1980) 303.

[9] CAMPBELL, D., CHEETHAM, A.D., CORDEY, J.G., et al., Bull. Am. Phys. Soc. **34** 2056.

[10] KOLESNICHENKO, Ya. I., REZNIK, S.N., YAVORSKY, V.A., The currents generated by α-particle loss in tokamak reactions, Nuclear Fusion **20** (**8**) (1980) 1041.

[11] PORCELLI, F., BERK, H. L., ZHANG, Y. Z., Internal kink stabilization of high energy ions with non-standard orbits, JET Report P(91)35 (1991).

[12] WHITE, R., BUSSAC, M.N., and ROMANELLI, F., Phys. Rev. Lett. **62** (1989) 539.

[13] EDERY, D., GARBET, X., ROUBIN, J.-P., et al, Variational formalism for kinetic-MHD instabilities in tokamaks CEA Report EUR-CEA-FC-1393.

[14] O'ROURKE, J., BLUM, J., CORDEY, J.G., et al., Polarimetric measurements of the q-profile, 15th European Conference on Controlled Fusion and Plasma Heating, **I** (1988)155.

TABLE I

Plasma Parameters

Major radius, R_0	2.96m
Minor radius, a	1.20m
Electron density on axis, $n_e(o)$	$5x10^{19}m^{-3}$
Electron density profile parameter	0.5
Electron temperature on axis, $T_e(o)$	10keV
Electron temperature profile parameter	6
Magnetic field at $R = R_0$, B_ϕ	3.4T
Plasma current, I_p	3.5MA
^3He minority concentration, $n_{^3He}/ne$	5%
Electric field profile parameter, L	0.2m
Perpendicular wave vector $k_\perp$	0
Parallel wave vector $k_\parallel$	$7m^{-1}$
Frequency, f	33MHz
Input power, P_{IN}	12MW

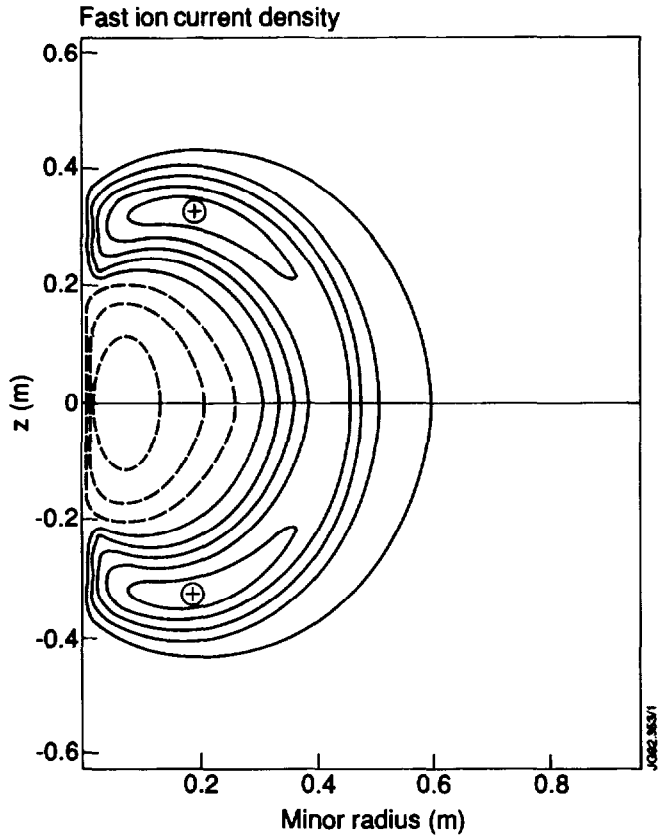

Fig. 1 Result of a semi-analytical calculation of the fast ion current density profile displayed as a contour map. The contour levels of constant fast ion current density (in units of MA / m^2) are at: -0.75, -0.45, -0.15, 0.15, 0.45, 0.75, 1.05 and 1.35. Negative current densities are indicated by the dashed contours.

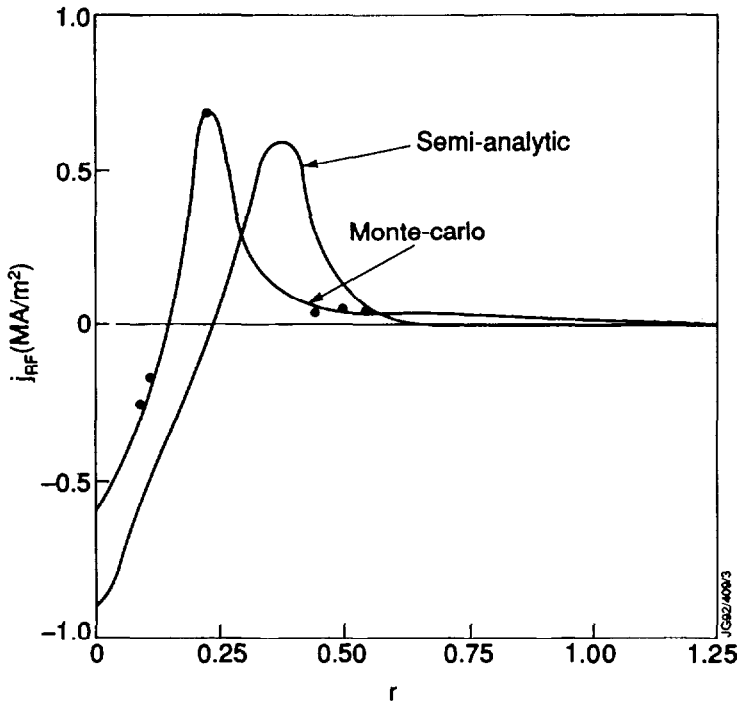

Fig. 2 The flux-surface averaged fast ion current density for a Monte-Carlo calculation and a semi-analytical model. Finite orbit effects give rise to two concentrations of current density. The (+) current density peak ($j_{max} \sim 0.7MA/m^2$) at $r/a = 0.22$ is in the direction of the plasma current. The (-) current density is in the direction opposite to the plasma current.

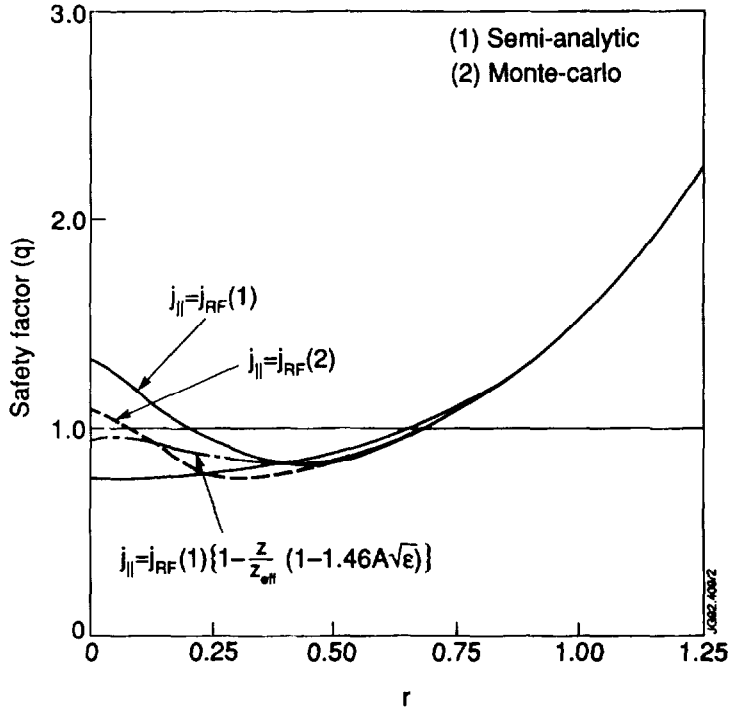

Fig. 3 The effect of the fast ion current on the q-profile. The full line is calculated using the current density profile $j(r) = j(0)(1 - (r/a)^2)^{5/2}$. The addition of the non-inductive component increases the on-axis value $q(0)$ and leads to the flattening of the q-profile where $dq/dr = 0$. Typical experimental parameters were assumed with $Z = 2$, $Z_{eff} = 3.5$, and $A = 1.0$.

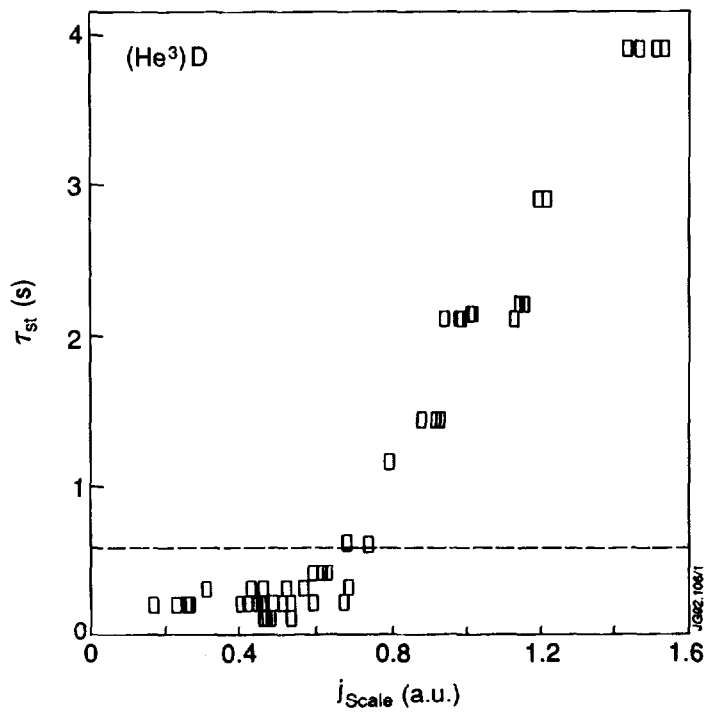

Fig. 4 The sawtooth-free period τ_{st} plotted as a function of the fast ion current scaling $j_{scale} \propto n\, Z_f\, v\, \rho_\theta^{1/3}$ for JET (He^3) D ICR heating data. The horizontal dashed line is at $\tau_{st} = 0.6$ sec, the criterion (in JET) above which the sawteeth are considered to be stabilised.

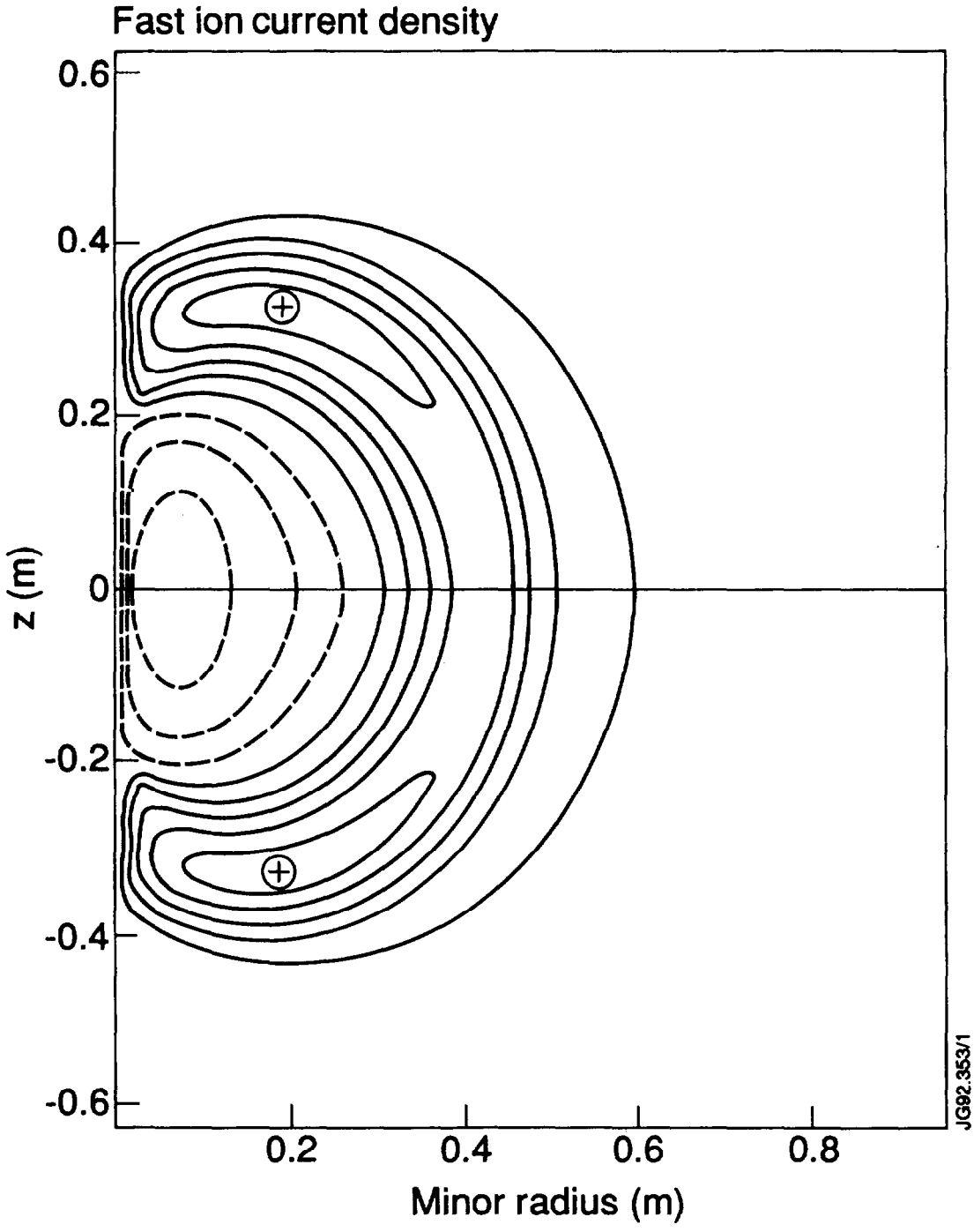
Fast ion current density
0.6
0.4
0.2
0
-0.2
-0.4
-0.6
z (m)
0.2
0.4
0.6
0.8
Minor radius (m)
JG92.353/1

Fig 1

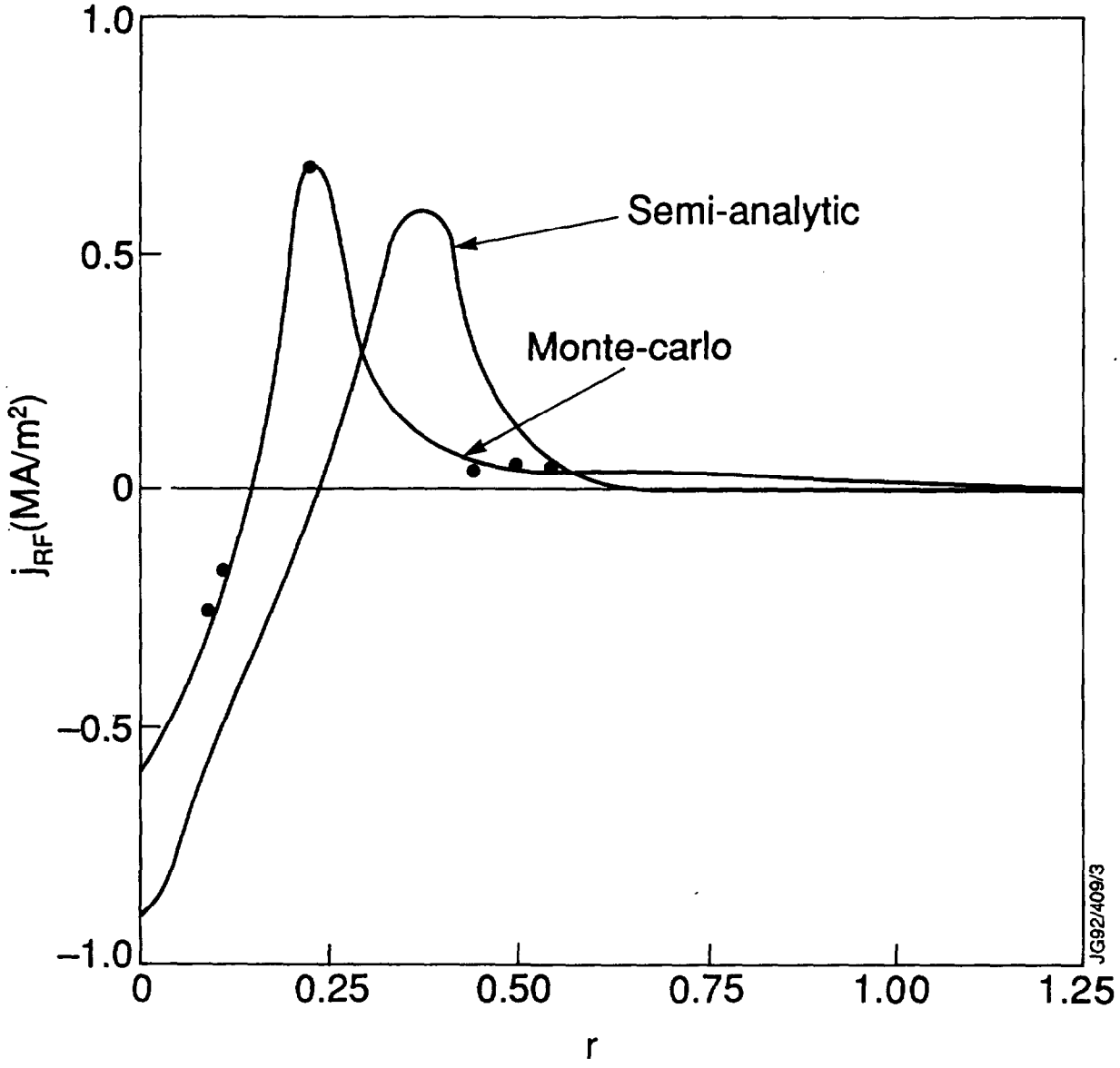
1.0
0.5
0
−0.5
−1.0
j_{RF}(MA/m²)
Semi-analytic
Monte-carlo
0
0.25
0.50
0.75
1.00
1.25
r
JG92/409/3

Fig 2

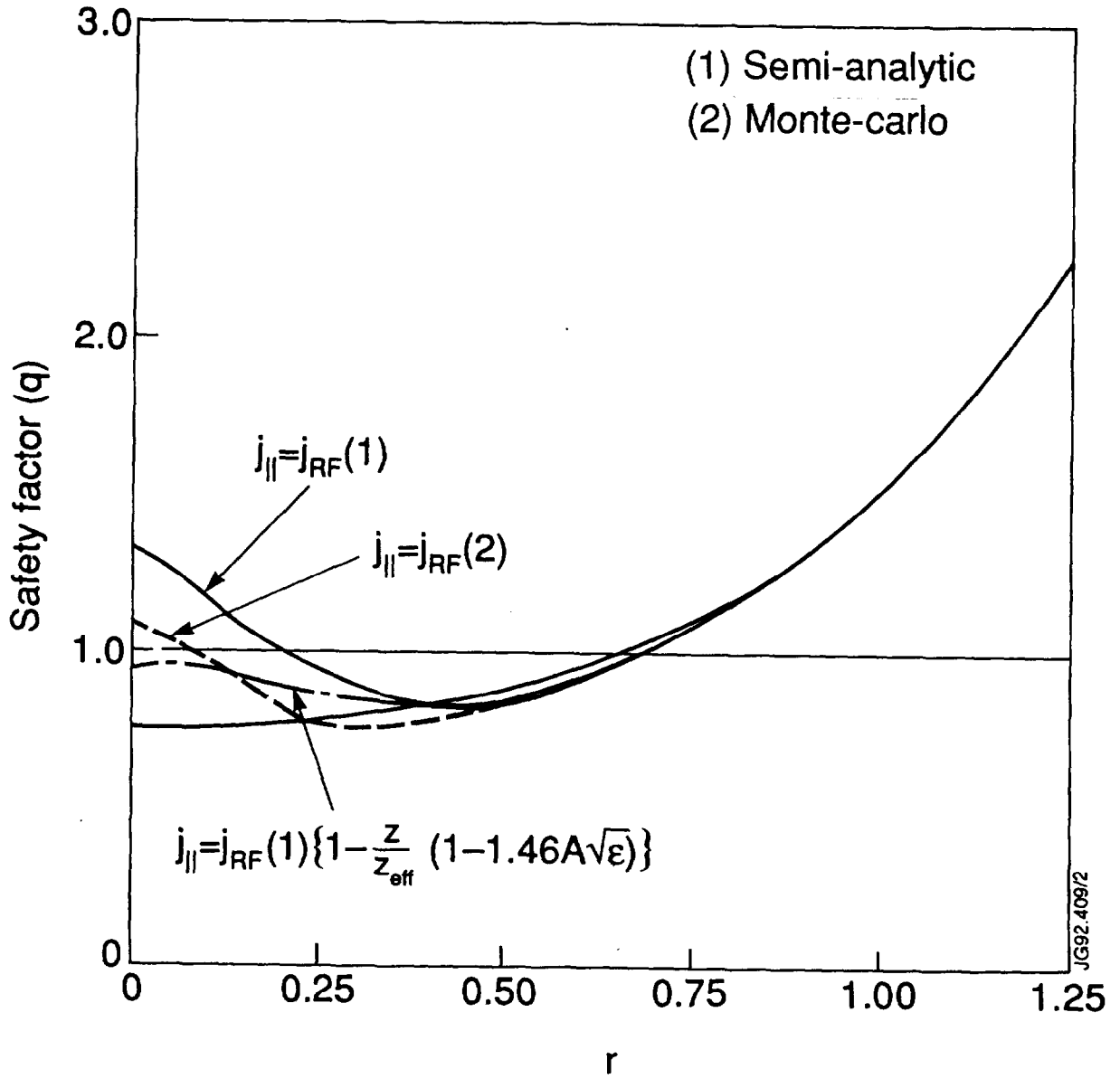
3.0
2.0
1.0
0
Safety factor (q)
(1) Semi-analytic
(2) Monte-carlo
$j_{||}=j_{RF}(1)$
$j_{||}=j_{RF}(2)$
$j_{||}=j_{RF}(1)\{1-\frac{Z}{Z_{eff}}(1-1.46A\sqrt{\varepsilon})\}$
JG92.409/2
0
0.25
0.50
0.75
1.00
1.25
r

Fig 3

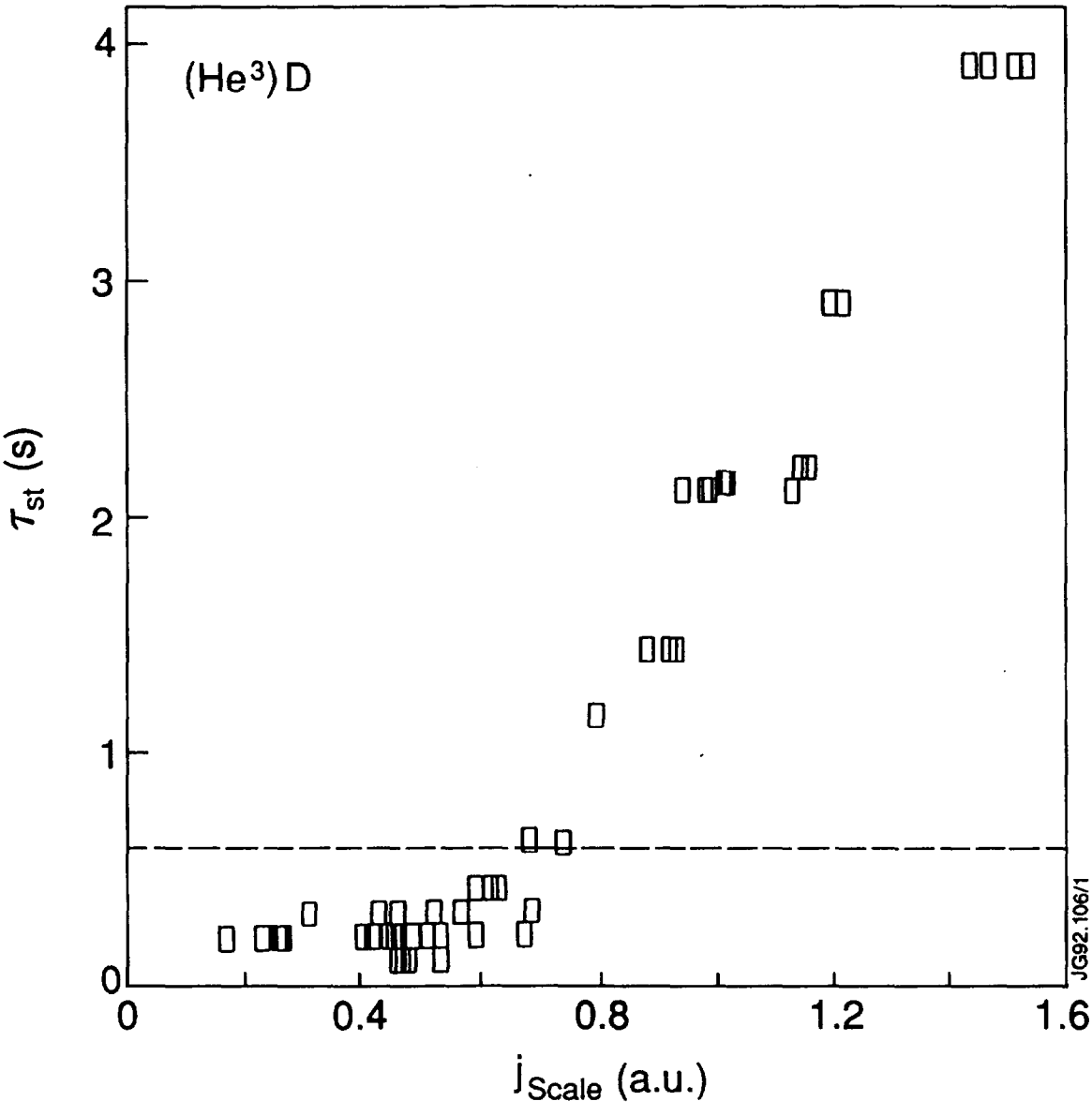

Fig 4.

ANNEX

P.-H. REBUT, A. GIBSON, M. HUGUET, J.M. ADAMS[1], B. ALPER, H. ALTMANN, A. ANDERSEN[2], P. ANDREW[3], M. ANGELONE[4], S. ALI-ARSHAD, P. BAIGGER, W. BAILEY, B. BALET, P. BARABASCHI, P. BARKER, R. BARNSLEY[5], M. BARONIAN, D.V. BARTLETT, L. BAYLOR[6], A.C. BELL, G. BENALI, P. BERTOLDI, E. BERTOLINI, V. BHATNAGAR, A.J. BICKLEY, D. BINDER, H. BINDSLEV[2], T. BONICELLI, S.J. BOOTH, G. BOSIA, M. BOTMAN, D. BOUCHER, P. BOUCQUEY, P. BREGER, H. BRELEN, H. BRINKSCHULTE, D. BROOKS, A. BROWN, T. BROWN, M. BRUSATI, S. BRYAN, J. BRZOZOWSKI[7], R. BUCHSE[22], T. BUDD, M. BURES, T. BUSINARO, P. BUTCHER, H. BUTTGEREIT, C. CALDWELL-NICHOLS, D.J. CAMPBELL, P. CARD, G. CELENTANO, C.D. CHALLIS, A.V. CHANKIN[8], A. CHERUBINI, D. CHIRON, J. CHRISTIANSEN, P. CHUILON, R. CLAESEN, S. CLEMENT, E. CLIPSHAM, J.P. COAD, I.H. COFFEY[9], A. COLTON, M. COMISKEY[10], S. CONROY, M. COOKE, D. COOPER, S. COOPER, J.G. CORDEY, W. CORE, G. CORRIGAN, S. CORTI, A.E. COSTLEY, G. COTTRELL, M. COX[11], P. CRIPWELL[12], O. Da COSTA, J. DAVIES, N. DAVIES, H. de BLANK, H. de ESCH, L. de KOCK, E. DEKSNIS, F. DELVART, G.B. DENNE-HINNOV, G. DESCHAMPS, W.J. DICKSON[13], K.J. DIETZ, S.L. DMITRENKO, M. DMITRIEVA[14], J. DOBBING, A. DOGLIO, N. DOLGETTA, S.E. DORLING. P.G. DOYLE, D.F. DÜCHS, H. DUQUENOY, A. EDWARDS, J. EHRENBERG, A. EKEDAHL, T. ELEVANT[7], S.K. ERENTS[11], L.G. ERIKSSON, H. FAJEMIROKUN[12], H. FALTER, J. FREILING[15], F. FREVILLE, C. FROGER, P. FROISSARD, K. FULLARD, M. GADEBERG, A. GALETSAS, T. GALLAGHER, D. GAMBIER, M. GARRIBBA, P. GAZE, R. GIANNELLA, R.D. GILL, A GIRARD, A. GONDHALEKAR, D. GOODALL[11], C. GORMEZANO, N.A. GOTTARDI, C. GOWERS, B.J. GREEN, B. GRIEVSON, R. HAANGE, A. HAIGH, C.J. HANCOCK, P.J. HARBOUR, T. HARTRAMPF, N.C. HAWKES[11], P. HAYNES[11], J.L. HEMMERICH, T. HENDER[11], J. HOEKZEMA, D. HOLLAND, M. HONE, L. HORTON, J. HOW, M. HUART, I. HUGHES, T.P. HUGHES[10], M. HUGON, Y. HUO[16], K. IDA[17], B. INGRAM, M. IRVING, J. JACQUINOT, H. JAECKEL, J.F. JAEGER, G. JANESCHITZ, Z. JANKOVICZ[18], O.N. JARVIS, F. JENSEN, E.M. JONES, H.D. JONES, L.P.D.F. JONES, S. JONES[19], T.T.C. JONES, J.-F. JUNGER, F. JUNIQUE, A. KAYE, B.E. KEEN, M. KEILHACKER, G.J. KELLY, W. KERNER, A. KHUDOLEEV[21], R. KONIG, A. KONSTANTELLOS, M. KOVANEN[20], G. KRAMER[15], P. KUPSCHUS, R. LÄSSER, J.R. LAST, B. LAUNDY, L. LAURO-TARONI, M. LAVEYRY, K. LAWSON[11], M. LENNHOLM, J. LINGERTAT[22], R.N. LITUNOVSKI, A. LOARTE, R. LOBEL, P. LOMAS, M. LOUGHLIN, C. LOWRY, J. LUPO, A.C. MAAS[15], J. MACHUZAK[19], B. MACKLIN, G. MADDISON[11], C.F. MAGGI[23], G. MAGYAR, W. MANDL[22], V. MARCHESE, G. MARCON, F. MARCUS, J. MART, D. MARTIN, E. MARTIN, R. MARTIN-SOLIS[24], P. MASSMANN, G. MATTHEWS, H. McBRYAN, G. McCRACKEN[11], J. McKIVITT, P. MERIGUET, P. MIELE, A. MILLER, J. MILLS, S.F. MILLS, P. MILLWARD, P. MILVERTON, E. MINARDI[4], R. MOHANTI[25], P.L. MONDINO, D. MONTGOMERY[26], A. MONTVAI[27], P. MORGAN, H. MORSI, D. MUIR, G. MURPHY, R. MYRNÄS[28], F. NAVE[29], G. NEWBERT, M. NEWMAN, P. NIELSEN, P. NOLL, W. OBERT, D. O'BRIEN, J. ORCHARD, J. O'ROURKE, R. OSTROM, M. OTTAVIANI, M. PAIN, F. PAOLETTI, S. PAPASTERGIOU, W. PARSONS, D. PASINI, D. PATEL, A. PEACOCK, N. PEACOCK[11], R.J.M. PEARCE, D. PEARSON[12], J.F. PENG[16], R. PEPE DE SILVA, G. PERINIC, C. PERRY, M. PETROV[21], M.A. PICK, J. PLANCOULAINE, J.-P POFFÉ, R. PÖHLCHEN, F. PORCELLI, L. PORTE[13], R. PRENTICE, S. PUPPIN, S. PUTVINSKII[8], G. RADFORD[30], T. RAIMONDI, M.C. RAMOS DE ANDRADE, R. REICHLE, J. REID, S. RICHARDS, E. RIGHI, F. RIMINI, D. ROBINSON[11], A. ROLFE, R.T. ROSS, L. ROSSI, R. RUSS, P. RUTTER, H.C. SACK, G. SADLER, G. SAIBENE, J.L. SALANAVE, G. SANAZZARO, A. SANTAGIUSTINA, R. SARTORI, C. SBORCHIA, P. SCHILD, M. SCHMID, G. SCHMIDT[31], B. SCHUNKE, S.M. SCOTT, L. SERIO, A SIBLEY, R. SIMONINI, A.C.C. SIPS, P. SMEULDERS, R. SMITH, R. STAGG, M. STAMP, P. STANGEBY[3], R. STANKIEWICZ[32], D.F. START, C.A. STEED, D. STORK, P.E. STOTT, P. STUBBERFIELD, D. SUMMERS, H. SUMMERS[13], L. SVENSSON, J.A. TAGLE[33], M. TALBOT, A. TANGA, A. TARONI, C. TERELLA, A TERRINGTON, A TESINI, P.R. THOMAS, E. THOMPSON, K. THOMSEN, F. TIBONE, A. TISCORNIA, P. TREVALION, B. TUBBING, P. VAN BELLE, H. VAN DER BEKEN, G. VLASES, M. VON HELLERMANN, T. WADE, C. WALKER, R. WALTON[31], D. WARD, M.L. WATKINS, N. WATKINS, M.J. WATSON, S. WEBER[34], J. WESSON, T.J. WIJNANDS, J. WILKS, D. WILSON, T. WINKEL, R. WOLF, D. WONG, C. WOODWARD, Y. WU[35], M. WYKES, D. YOUNG, I.D. YOUNG, L. ZANNELLI, A. ZOLFAGHARI[19], W. ZWINGMANN

[1] Harwell Laboratory, UKAEA, Harwell, Didcot, Oxfordshire, UK.
[2] Risø National Laboratory, Roskilde, Denmark.
[3] Institute for Aerospace Studies, University of Toronto, Downsview, Ontario, Canada.
[4] ENEA Frascati Energy Research Centre, Frascati, Rome, Italy.
[5] University of Leicester, Leicester, UK.
[6] Oak Ridge National Laboratory, Oak Ridge, TN, USA.
[7] Royal Institute of Technology, Stockholm, Sweden.
[8] I.V. Kurchatov Institute of Atomic Energy, Moscow, Russian Federation.
[9] Queens University, Belfast, UK.
[10] University of Essex, Colchester, UK.
[11] Culham Laboratory, UKAEA, Abingdon, Oxfordshire, UK.
[12] Imperial College of Science, Technology and Medicine, University of London, London, UK.
[13] University of Strathclyde, Glasgow, UK.
[14] Keldysh Institute of Applied Mathematics, Moscow, Russian Federation.
[15] FOM-Institute for Plasma Physics "Rijnhuizen", Nieuwegein, Netherlands.
[16] Institute of Plasma Physics, Academia Sinica, Hefei, Anhui Province, China.
[17] National Institute for Fusion Science, Nagoya, Japan.
[18] Soltan Institute for Nuclear Studies, Otwock/Świerk, Poland.
[19] Plasma Fusion Center, Massachusetts Institute of Technology, Boston, MA, USA.
[20] Nuclear Engineering Laboratory, Lappeenranta University, Finland.
[21] A.F. Ioffe Physico-Technical Institute, St. Petersburg, Russian Federation.
[22] Max-Planck-Institut für Plasmaphysik, Garching, Germany.
[23] Department of Physics, University of Milan, Milan, Italy.
[24] Universidad Complutense de Madrid, Madrid, Spain.
[25] North Carolina State University, Raleigh, NC, USA.
[26] Dartmouth College, Hanover, NH, USA.
[27] Central Research Institute for Physics, Budapest, Hungary.
[28] University of Lund, Lund, Sweden.
[29] Laboratorio Nacional de Engenharia e Tecnologia Industrial, Sacavem, Portugal.
[30] Institute of Mathematics, University of Oxford, Oxford, UK.
[31] Princeton Plasma Physics Laboratory, Princeton University, Princeton, NJ, USA.
[32] RCC Cyfronet, Otwock/Świerk, Poland,
[33] Centro de Investigaciones Energéticas, Medioambientales y Tecnológicas, Madrid, Spain.
[34] Freie Universität, Berlin, Germany.
[35] Insitute for Mechanics, Academia Sinica, Beijing, China.